ORIGINAL ARTICLE

Identification of components from distant fibers in a recorded single muscle fiber potential (SFP) — a new approach to the SFP criteria

Ewa Zalewska[a], Malgorzata Gawel[b],*

[a] *Nalecz Institute of Biocybernetics and Biomedical Engineering, Polish Academy of Sciences, Ks. Trojdena 4 str., 02-109 Warsaw, Poland*
[b] *Department of Neurology, Medical University of Warsaw, Banacha 1A str., 02-097 Warsaw, Poland*

Summary
Objectives. — The aim of our study was to verify the effectiveness of single fiber potential (SFP) criteria in cases when the potential recorded using single fiber electrode (SFE) or concentric needle electrode (CNE) is contaminated by distant fibers.
Methods. — Morphological counterparts of SFP were studied using computer simulations. In this study, we examined triphasic potentials using a model of a linear source of SFP. The criteria defining SFP in the case of SFP contaminated by distant fibers were analyzed, and the effect of second fiber contamination on jitter and fiber diameter determination evaluated.
Results. — We found that SFP criteria prevent detection of SFP from fibers smaller than about 30 μm in diameter, but do not prevent classification of a potential as an SFP even though it is formed by two or more fibers. This suggests that the presently used criteria may lead to incorrect interpretation of SFP potentials. SFPs contaminated by fibers of diameters differing by a few percent fulfill the criteria but a negative peak may be shifted in time and therefore impact jitter and diameter measurements. This contamination generally tends to decrease both the jitter and the determined diameter. A new approach to the identification of SFP is presented, determining fiber diameter and distance from the electrode to enable maximum sensitivity to potential contamination by the effect of a second fiber.
Conclusion. — A new parameter characterizing SFP shape changes is introduced. This parameter is used in the method by which additional fibers affecting the SFP may be detected.
© 2018 Elsevier Masson SAS. All rights reserved.

* Corresponding author.
  E-mail address: mgawel@wum.edu.pl (M. Gawel).

Introduction

Single-fiber EMG (SFEMG) is of proven importance in the diagnosis of neuromuscular disorders, and is a valuable procedure for studying physiological and morphological parameters of the motor unit [8]. The most important diagnostic usefulness of SFEMG is to evaluate jitter and neuromuscular transmission as well as fiber density [7,13,28]. Jitter is the main subject of interest of the present study.

SFEMG during voluntary contraction is especially useful in myasthenia gravis in detecting abnormalities in neuromuscular transmission. In generalized myasthenia gravis, with weakness of all muscles, SFEMG shows impaired neuromuscular transmission in 95—99% of patients [2,10,24], while repetitive nerve stimulation (RNS) is abnormal in 76% patients with this type [15]. In ocular myasthenia gravis with selective muscle weakness involving the extraocular muscles, the levator palpebrae superioris, and the orbicularis oculi with symptoms and signs of diplopia and/or ptosis, SFEMG in the study by Padua et al. showed the highest sensitivity (100%) [15], while the sensitivity of repetitive nerve stimulation (RNS) in this type of myasthenia gravis was only 48% [23].

SFEMG measures jitter using a specially constructed single fiber electrode (SFE) containing an insulated platinum wire (diameter 25 μm) with a small recording surface to provide a point-size recording area that enables recording the activity of a single muscle fiber [14,23]. In contrast to reusable SFE, disposable concentric needle electrode (CNE), which is presently used for jitter measurement, mainly due to its low cost, has a much larger uptake area and therefore is less selective [26]. The problem of the possible contamination of additional fiber potentials when using CNE and how it may affect the result of the jitter was considered by Stålberg and Sanders [26]. The authors indicated that jitter values measured using CNE correlate with SFEMG values, but are reduced by a few microseconds [26,31]. This phenomenon was explained using computer simulations that showed that in the case of several potentials arriving at the electrode during consecutive discharges, they may be SFP of different muscle fibers and the earliest will be detected, thus decreasing the apparent jitter [26]. The results must be interpreted with caution, particularly in borderline cases [26].

Along the same lines, another question is whether the potential recorded using SFE is from a single fiber only or is contaminated by potentials from other fibers, as this may influence interpretation of the results [18,19,21,29,31,32].

Recognition of contaminated potentials recorded using either SFE or CNE requires morphological analysis. The shape of the recorded signal depends on the geometrical relationship between the fibers and the temporal dispersion of their action potentials. SFP parameters such as amplitude and duration are currently not widely useful clinically, although their changes related to fiber diameter and the electrode to fiber distance have been established in simulation studies [14,18,19,21]. The rise-time of a single fiber action potential should be limited to a predefined range to assure that the electrode is placed close to the single fiber. When the rise time of the potential is greater than the range, there is the possibility that it is formed by summation of the potentials generated by fibers belonging to the same motor unit [8,28].

A new approach for practical application of SPFs shape analysis, i.e., a method for the determination of fiber properties from the analysis of its SFP, has been proposed by Zalewska et al. [32,33] This practical and easy to use analytical and graphical method involves determination of muscle fiber diameter as a quantity related to the duration of the negative SFP peak.

Morphological counterparts of SFP parameters were studied using computer simulations. Rodriguez et al., analysed the shape variability caused by contribution of other fibers and the possible impact on the jitter measurement [20]. Zalewska and Gawel showed that contamination of the recorded single fiber potential with distant fiber potentials results in reduction of the measured jitter [31]. The jitter measured from summated signals may be less than that measured from individual action potentials (if the time intervals are measured to the earliest part of the signal, which is produced by whichever first contributing action potential) or it may be greater (if the disturbing signal affects the measuring point of the signal peak) [22,29].

Simulation analysis of SFP indicated another issue that may be important in the practice of SFEMG [32], namely identifying contribution of other fibers to the recorded SFP and verifying whether the contaminated potentials fulfill the criteria defined for the identification of SFP defined by Stålberg and used in the practice of SFEMG [30].

The criteria for the SFP parameters have been defined as follows [22].

The recorded potential is considered as resulting from a single fiber (single fiber potential, SFP) by using the following criteria:

(a) amplitude range 200 μV—20 mV;
(b) rise time of ≤ 0.3 ms;
(c) the recorded potential is also filtered using a band pass filter which typically ranges from 500 Hz to 10 kHz. The filter is used to eliminate the effect of distant fibers;
(d) a rule that the obtained potential must resemble a single fiber potential in that it has no extra phases or turns.

The aim of the present study was to analyze the effectiveness of these criteria using the simulation method in cases when a recorded SFP is contaminated by potentials from other fibers, and to evaluate the effect of this contamination on the jitter measurement and determination of muscle fiber diameter. The aim was also to extend the SFP criteria, to allow verification whether the recorded SFP is a single muscle fiber potential, or contaminated by another fiber potential.

Methods

The current simulation studies were performed using the model of a linear source of a muscle fiber potential proposed by Nandedkar and Stålberg [14], because its properties are well understood and are consistent with the results of experimental measurements [5]. Nandedkar and Stålberg [14] have shown a high agreement between parameters of

modeled potentials and physiological measurements with respect to the linear relationship of amplitude versus diameter and amplitude versus propagation velocity [14]. The reliability of the linear source model has been confirmed in several studies on the correlation between muscle morphology and function and is consistent with the knowledge in the field of clinical electromyography [1,3].

In this study, we have focused on three-phasic potentials using a model of the linear source of SFP. We have not analysed biphasic potentials. Biphasic potentials are usually recorded when the needle is very close to the end-plate and their shape depends very sensitively on the distance and filter used. Because of this, biphasic potentials are not suitable for our analysis and from the recorded set of potentials we selected only triphasic ones for further analysis. Biphasic potentials were described, analysed and simulated by Rodriguez et al. [17] and Dumitru et al. [6] (see these references for further detail).

In the case of triphasic potentials, the needle is at a sufficient distance from the end-plate so that the shape of the potential is stable. If the waveform begins some distance from the needle, there is an initial deflection as it moves towards the needle, followed by a negative phase as it moves beneath the needle, and then a final positive deflection as it travels away. A traveling depolarizing wave will create a biphasic potential if the waveform begins under the recording needle electrode (initial negative peak) and then moves away from the electrode (positive peak) [16]. Triphasic potentials are better suited to fiber diameter determination, which was our main aim in this study.

SFP model and parameters

Simulated SFPs have been calculated using the formulation given by Nandedkar and Stålberg, assuming the same values of tissue conductance and current propagation velocity [14]. In the models, the end-plate zone to electrode distance was assumed to be 25 mm. The sampling frequency was set at 48 kHz, corresponding to that used in the EMG equipment. A Butterworth second order filter with cutoff frequencies 500 Hz—10 kHz (consistent with standard settings in the apparatus) was used to filter the simulated potentials.

A series of SFPs for different fiber diameters as well as for a set of fiber to electrode distances was calculated. For each calculated model (SFP), we calculated the standard set of parameters viz. amplitude, area, Size Index (SI), Negative Peak Duration (NPD), rise time, and the number of phases and turns.

SFP contamination by other fibers

In order to examine whether the SFP criteria (a) through (d) enable to select a potential from a single fiber, we calculated SFP for a selected fiber diameter and then added an additional fiber at distances ranging from 1 mm from the electrode (distant fiber) to the distance of the principal fiber. By moving the second fiber from a large distance to the same distance from the electrode as the principal fiber, we were able to examine the effect of the contamination.

The second fiber diameter was chosen in such a way that the resulting potential should have no additional phases and turns, i.e., the peaks should not separate. For each studied fiber diameter, we determined a range of allowable second fiber diameters such that the resulting potential would be smooth and look like a SFP.

Results

Analysis of the criteria defining SFP: the amplitude range of SFP

The method of fiber diameter and fiber to electrode distance derivation from SFP amplitude and NPD was presented by Zalewska et al. [32]. The amplitudes obtained using this method from the SFP models are presented in Fig. 1 for several fiber diameters and fiber to electrode distances.

Fig. 1 shows that with the assumed amplitude range (0.2 mV to 2 mV) [28] defining the SFP, potentials from fibers that are more distant from the electrode than about 350 μm would be rejected. Therefore, the amplitude criterion eliminates distant fibers.

From the graph it can be seen that for most of the range of the considered fiber diameters (15 μm—95 μm) and fiber to electrode distances (1 μm—350 μm), the calculated SFP amplitudes are consistent with the range indicated in the criteria [30]. However, for larger fibers (with diameters ≥ 60 μm) which happen to be close to the electrode, the amplitude criterion would eliminate them (as potentials with amplitudes that are too large). Also, potentials from fibers smaller than 60 μm located further than about 200 μm away from the electrode would be eliminated. Hence, the amplitude criterion would tend to eliminate potentials from small fibers that are not close enough to the electrode.

It is worth noting that, while the amplitude criterion eliminates cases when a single fiber is far from the electrode, it does not eliminate cases where a potential from a fiber close to the electrode is contaminated by a potential from a more distant fiber.
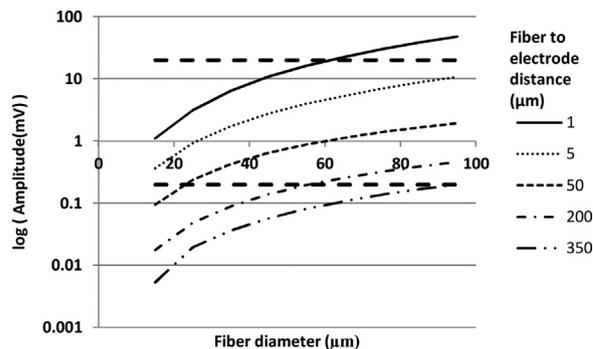
Figure 1 Dependence of the amplitude on the fiber diameter for a set of fixed fiber to electrode distances. For better readability, the range of amplitudes is shown using a logarithmic scale. The dashed lines represent the range of amplitudes assumed for SFP.
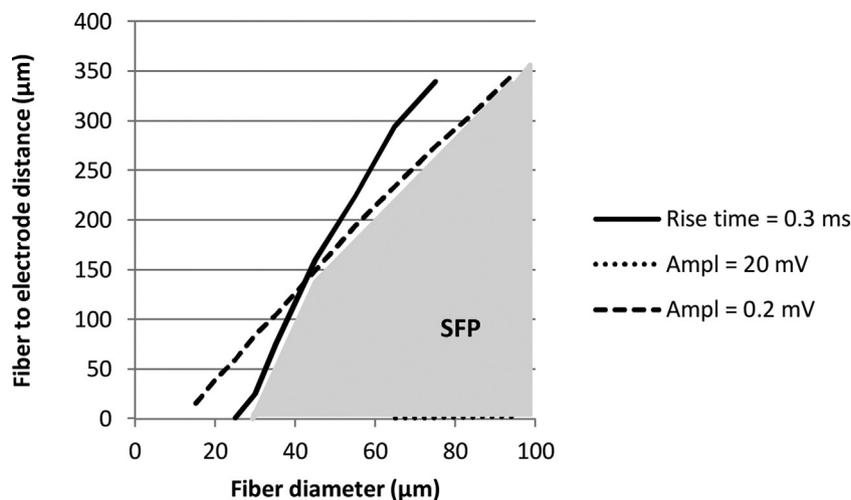
Figure 2 The limits of fiber diameter and fiber to electrode distance obtained by using the criteria for amplitude and rise time of a SFP. The gray area marks the range of parameters where the potential will be classified as SFP.

Analysis of the criteria defining SFP: the rise time of SFP

The criterion of rise time limits the range of fiber diameters and fiber to electrode distances for which a measured potential will be classified as SFP. From Fig. 1 it can be seen that the maximal distance for a given fiber diameter is defined by the crossing point with the horizontal line for the amplitude = 0.2 mV. The resulting, nearly linear dashed curve is shown in Fig. 2. Similarly, a curve may be obtained corresponding to the amplitude equal to the 20 mV limit (dotted curve). In the same way, a curve representing the criterion of rise time ≤ 0.3 ms may be obtained. These curves are shown in Fig. 2.

The range of fiber diameters and fiber to electrode distances between the curves corresponding to the amplitude limits and below the rise time limit curve determines the region on the graph (shaded area) where a potential would be classified as SFP.

As may be seen from the graph, the rise time criterion eliminates fibers smaller than about 35 μm. A fiber with a diameter of 35 μm would have to be closer to the electrode than a 75 μm one while a fiber with a diameter of 30 μm would have to be closer than a 25 μm one. Fibers smaller than about 30 μm would be rejected by the rise time criterion. For fibers larger than about 50 μm, the criterion of amplitude ≥ 0.2 mV is more stringent than the rise time criterion.

From the data it follows that for fibers larger than about 40 μm, they can be located at some distance from the electrode − from about 120 μm for a 40 μm fiber to more than 300 μm for large fibers (diameter of 90 μm) and they will still be classified as SFP.

However, the criteria do not allow fibers smaller than about 35 μm to be detected.

It should be noted that the results presented in Figs. 1 and 2 are for potentials filtered using the band pass filter. The area of detectability of the SFP would be different should another filter be used.

Effect of contamination by a second fiber on the determination of SFP parameters

As can be seen from Fig. 2, a fiber giving rise to a SFP may be quite distant, up to about 350 μm. With an increase in the fiber to electrode distance, there is a greater probability of finding another fiber which may contribute to the recorded potential, thus contaminating it. Usually, during the examination the needle is rotated or moved in such a way as to obtain the largest signal amplitude. This means that the electrode is closest to a certain fiber in the motor unit. However, another fiber in the motor unit may be within the scoop range of the electrode and thus have a contaminating effect on the recorded potential.

An example of a contaminated SFP is shown in Fig. 3. The thick solid curve represents the potential obtained from two fibers located at a distance of 50 μm from the electrode and differing by 1 μm in diameter viz. one fiber has a diameter of 55 μm and the other 56 μm. As can be seen from
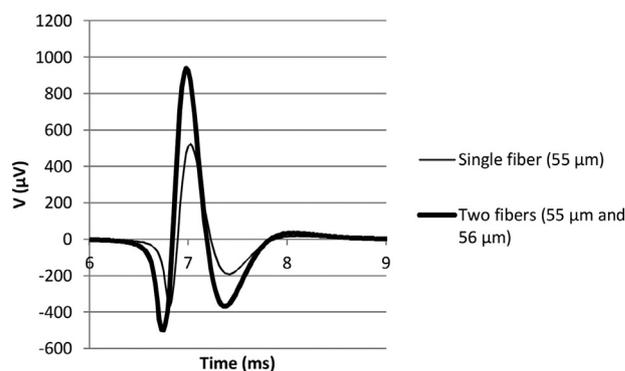
Figure 3 A potential resulting from two fibers (with diameters 55 μm and 56 μm) located at the distance of 50 μm from the electrode (thick solid curve) compared to SFP from a fiber of diameter 55 μm located at the distance of 50 μm from the electrode. The two potentials look similar.
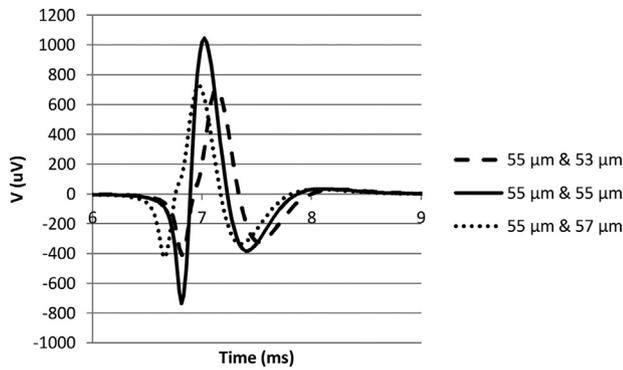
Figure 4 Comparison of two-fiber potentials from fibers close in diameter. The fibers are located 50 μm from the electrode.

Table 1 Range of second fiber diameter such that the resulting potential may be miss-classified as SFP.

First fiber diameter (μm)	Second fiber diameter (μm)	
	From	To
35	34.4	35.6
55	53.3	56.8
75	72.4	77.7
95	91.7	98.5

Figure 5 Potentials from pairs of fibers shifted in time and scaled so that the maxima of negative peaks coincide. The largest variability in scaled potentials occurs at the first minimum.

the figure, the two-fiber potential closely resembles a single fiber potential (curve marked with a thin line). In this case, the amplitude of the two-fiber potential is larger than that of a single fiber but both its amplitude and rise time are well within the limits. Since the two-fiber potential has no additional turns or phases, it could be easily mistaken for a SFP.

For a given fiber diameter of the single fiber potential, there is a certain range of the second fiber diameters such that the resulting potential appears indistinguishable from a SFP based on its amplitude and rise time as well as the number of phases and turns.

In a special case where two fibers have the same diameter, the resulting potential will fulfill the SFP criteria but will have twice the amplitude.

For two fibers differing in diameter, the resulting potential has a smaller amplitude. The peaks are time dispersed as illustrated in Fig. 4. In Fig. 4, the potential from two fibers with diameters of 55 μm is compared to the potentials from a fiber of 55 μm diameter accompanied by a second fiber with a diameter such that the resulting potential still does not have additional turns. For 55 μm diameter, the second fiber diameter must be within the range of 53 μm to 57 μm for the potential to resemble SFP.

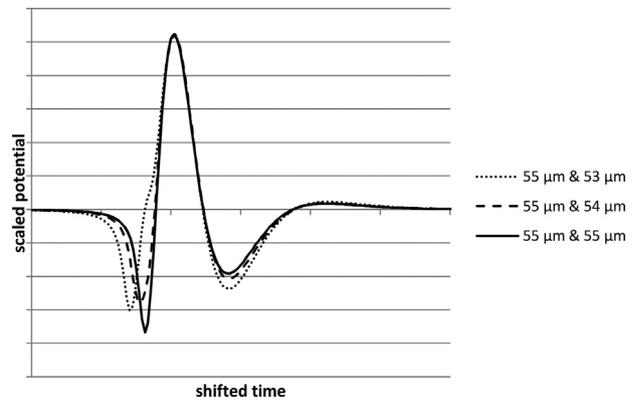As can be seen from Fig. 4, the potential from a fiber that is larger than 55 μm has its extrema shifted to an earlier time while the potential resulting from a fiber smaller than the main one is shifted towards longer times. The potentials resulting from a 55 μm fiber with the second fiber in between the limiting diameters lie between those two extreme potentials and have higher amplitudes.

The range of acceptable second fiber diameters for a few values of the first fiber diameter is given in Table 1. The range of second fiber diameters is in some cases limited by the requirement that no additional turns appear in the potential or by the rise time requirement. The latter is particularly strong for a small main fiber. For fibers with a diameter of 35 μm, the range of secondary fiber diameters is ±0.6 μm, while for large fibers this range is substantially larger.

From the data in Table 1, the range (in μm) of secondary fiber diameter may be approximately given by $d \pm 0.047 (d - 20)$ where d is the primary fiber diameter (in μm). A potential resulting from such two fibers looks like a SFP.

Due to the rise time criterion (see Fig. 2), the effect of a secondary fiber cannot be examined for fibers smaller than about 30 μm.

In order to examine in closer detail how the shape of the two-fiber potential changes depending on fiber diameters, the potentials seen in Fig. 4 were shifted in time and scaled so that their negative peaks coincided. The results are presented in Fig. 5.

From Fig. 5, it may be seen that the largest variability of the shape of the potential occurs at the first minimum. Both the relative amplitude of the first minimum as well as its location in time change. In case of the second minimum, there is also some variability of the amplitude although the location in time (i.e. distance in time from the negative peak) is more or less constant. Hence, it may be concluded that the presence of a second fiber affects mainly (except for amplitude) the first minimum of potential.

In Fig. 5, the potentials for the secondary fiber diameter larger than 55 μm are not shown as they overlap with those shown, i.e. the potential for 55 μm and 56 μm coincides with that for 55 μm and 54 μm while the one for 55 μm and 57 μm coincides with that for 55 μm and 53 μm. Thus, the change in the first minimum seems to be symmetric with respect to the difference between the first and the second fiber diameter. The change increases with an increase in the absolute difference between the second fiber diameter and the basic fiber diameter.
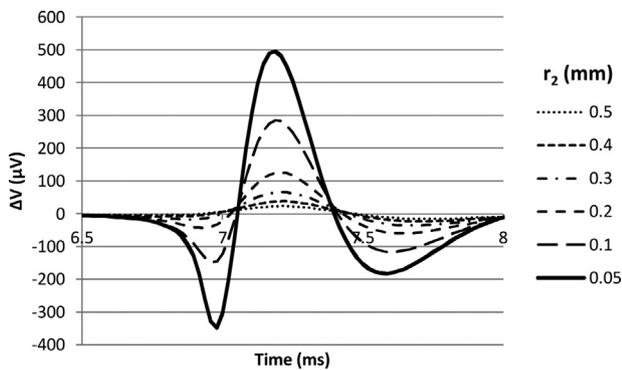
Figure 6 Difference of potentials from two fibers (55 μm and 53 μm) and from a single fiber (55 μm) for a range of second fiber to electrode distances (r_2): $\triangle V = V(\text{two fibers}) - V(\text{single fiber})$. The first fiber is at the distance of 0.05 mm from the electrode.

Range of contamination radius

In the preceding section, the second fiber was assumed to be at the same distance as the first (dominant) one. It may be expected that when the second fiber is moved away from the needle, then its effect on the potential will decrease.

This is illustrated in Fig. 6 where the difference of potentials (potential from two fibers minus potential from a single fiber) is shown for a range of second fiber distances from the electrode ranging from 50 μm to 500 μm.
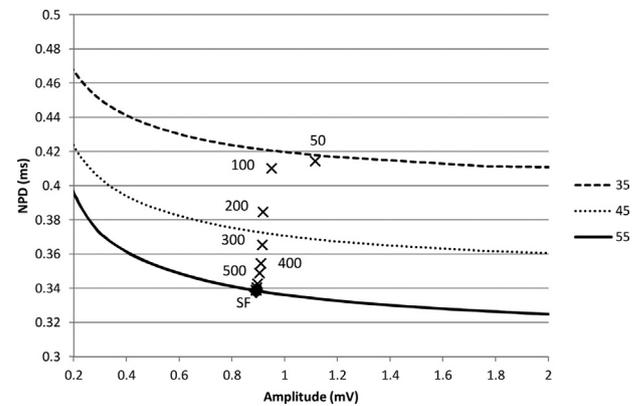
With the increase in the distance of the second fiber from the electrode, its effect on the potential decreases, i.e., the difference tends to zero. For a second fiber distance larger than about 750 μm, the difference in amplitudes is below 10 μV. This radius may be called the contamination radius.

Hence, the contaminating effect of the second fiber on the amplitude persists (for fiber diameter 55 μm) up to a distance much larger than the maximum distance of 350 μm allowed for a single fiber by the amplitude criterion (see Fig. 2). Thus, the scoop range for contaminating fibers is not limited by the criteria (a) through (d), and is much larger.

With such a large range of fiber to electrode distances at which it is possible that a second fiber would contaminate the SFP, it is quite probable that during routine examinations, situations when the potential is due to two or more fibers may quite commonly arise. For the average fiber density of ∼ 5 fibers/mm^2, it may be expected that there will be ∼ 4 fibers within a radius of ∼ 750 μm from the electrode. Thus, a method allowing determination whether a given recorded potential is due to a single fiber or comes from more fibers is necessary.

Influence on fiber diameter determination

In our paper (Zalewska et al. [32]), we have shown that by using amplitude and negative peak duration, it is possible to determine fiber diameter and fiber to electrode distance from a SFP. As has been shown in the preceding sections, contamination by a second fiber affects potential shape and amplitude and thus such a contamination will have an effect on the determined fiber diameter and fiber to electrode distance.

Figure 7 Determination of the fiber diameter from the potential amplitude and negative peak duration. The SF is the fiber diameter derived from a single fiber potential (55 μm diameter). The crosses are labeled with the distance of the second fiber from the electrode (in μm). The curves correspond to loci of amplitude-NPD dependence for fibers with diameters of 35, 45 and 55 μm.

In Zalewska et al. [32], it was shown that for the derivation of fiber diameter from SFP, a graph like Fig. 7 is useful. This graph enables to determine the fiber diameter from the measured amplitude and negative peak duration. The location of the point corresponding to a single fiber of 55 μm diameter is marked as diamond (and labeled SF). When a second fiber is introduced, the amplitude and negative peak duration of the potential change, and the size of this effect depends on the distance of the second fiber from the electrode. On the graph, crosses show how the second fiber affects diameter determination. The labels above the crosses denote the second fiber to electrode distance (in μm). The second fiber diameter was 53 μm in the case shown in Fig. 7.

Note that the behavior of the points on the graph depends on the fiber diameters used. For other fiber diameter combinations, location of the points may be quite different.

As may be seen, if the potential were due to two fibers with the diameters of 55 μm and 53 μm located at a distance of 50 μm from the electrode and it was assumed that it is a SFP, then the determined fiber diameter would be 35 μm, significantly, below the actual single fiber diameter of 55 μm. Hence, contamination of the potential by a second fiber would change the determined diameter by 20 μm.

With the increase of the second fiber to electrode distance, its effect on the determined fiber diameter diminishes. For second fiber distances larger than about 450 μm, the error in the determination of the fiber diameter falls below 5 μm which may be considered a reasonable level of accuracy.

This means that in order to have a significant effect on diameter determination, the contaminating second fiber should be closer to the electrode than about 450 μm. This may be called the practical contamination radius.

With normal fiber density, two fibers should be found within distance of 500 μm from the electrode. Since the practical contamination radius is smaller than that, the probability of finding a second fiber contaminating the SFP is smaller than one. From our calculations it follows that
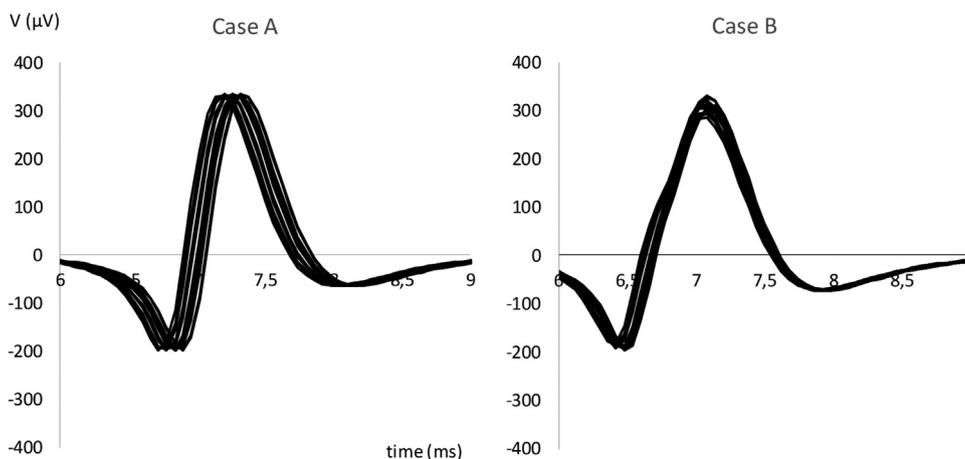
Figure 8 We have measured the jitter as the fluctuation of the position of the potential maximum (negative peak). For sequences A and B, we have calculated the average inter-potential intervals (MCD) as follows: $MCD = \frac{|IPI_2 - IPI_1| + \cdots + |IPI_n - IPI_{n-1}|}{n}$.

for typical fiber density there is a 60% chance of finding two fibers within 450 µm distance from the electrode. However, since when looking for SFP the electrode is manipulated in such a way that the signal is strongest, then it is probable that one fiber will be close to the electrode. Hence, the method of SFP selection is not random and in such a case, the probability that a second fiber is within 450 µm from the electrode, provided that the first one is closer than about 450 µm, is 88%. Therefore, it is quite probable in SFP measurements that a second fiber will be close enough to affect the recording and potential parameters.

Hence, an independent method for determination of the fiber diameter is required to allow confirmation based on the amplitude and negative peak duration.

Influence on jitter measurement

In order to estimate the effect of contamination of a single fiber potential by a second fiber on the measurements of jitter, we have performed the following modeling.

We have assumed that the main (triggering) potential is a real single fiber potential, i.e. it is due to a single fiber. For the secondary potential we have assumed two cases: case A — the secondary potential is due to a single fiber with a diameter of 40 µm, and case B — the secondary potential is due to two fibers with similar diameters. In case B, the first of the two fibers had a diameter of 40 µm, and the second one a diameter in the range from 40 µm to 46 µm.

In both cases, a sequence of secondary potentials was generated with an assumed jitter. In case A, for each potential in the sequence a value of jitter was chosen randomly from the assumed jitter range. In case B, the values of jitter for both fibers were independently selected from the assumed jitter range. In case B, only those resulting potentials that looked like SFP were included in the sequence. The resulting potentials in cases A and B are shown in Fig. 8.

We have performed simulations by assuming a level of jitter and performing calculations for case A and case B. In case B, a given value for the second fiber diameter was assumed and the calculated MCD_A and MCD_B was compared. In order to compare the effect of the second fiber in case B,

the ratio of MCD_B to MCD_A was calculated. The calculations were then repeated for a different second fiber diameter.

Fig. 9 summarizes the determined relation of MCD_B and MCD_A. In this figure, the ratio of MCD calculated for case A and case B is shown. As it may be seen, the ratio $^{MCBB}/_{MCDA}$ changes depending on the diameter of the contaminating fiber and the assumed level of jitter.

If the contaminating fiber did not have any effect on the measurement of jitter in Case B, then MCD_B would be similar to MCD_A and the ratio would be close to unity.

However, as can be seen from the figure, the ratio depends sensitively on the diameter of the contaminating fiber.

Even when the two fibers in case B have the same diameter (of 40 µm), the MCD for case B is lowered by about 30% relative to the single fiber case A. As can also be seen, this occurs for both small jitter ($MCD_A = 27$ µs) and for a larger one ($MCD_A = 67$ µs). When the second fiber diameter (in case B) is around 43 µm, the ratio approaches unity, but for small jitter level it exceeds unity by about 20% and for larger jitter level it is about 10% smaller than for the single fiber case A. For larger secondary fiber diameters, the MCD in case B decreases relative to case A and deviates significantly from unity (by up to 80%).

From the presented modeling example, it may be seen that the contamination of the secondary peak by an influence of a second fiber with a similar diameter has a significant effect on the measured jitter. The contamination generally tends to decrease the jitter by 30% to 80% in the case presented. In some cases, the jitter measured for a SFP, which is contaminated by a second fiber may be larger than that which would occur in a true single fiber potential.

New parameters to characterize SFP

The potential is characterized by a set of standard parameters like amplitude, area, size index, etc. For the purpose of the present study, we have introduced two new parameters: L/N and R/L. These parameters are defined as follows: L/N is equal to the ratio of the first minimum to the maximum (the negative peak) and R/L as the ratio of the right minimum
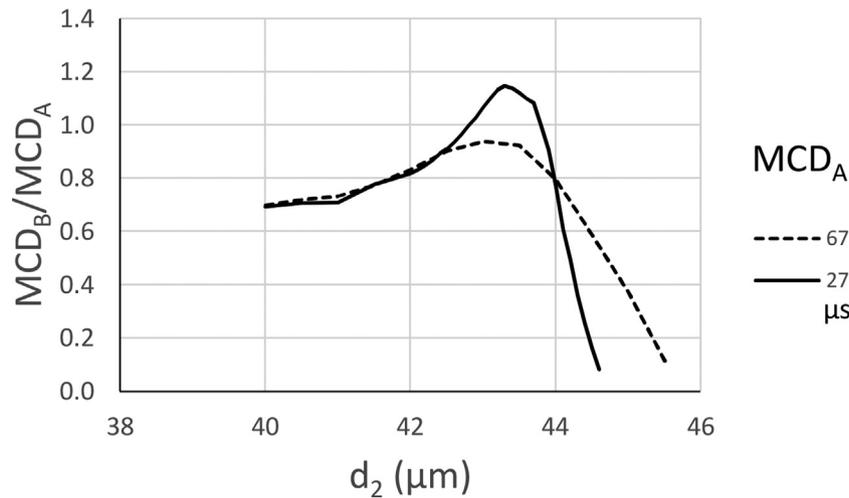
Figure 9   Ratio of inter-potential intervals for Case B and Case A for simulated potential sequences with jitter as a function of the second fiber diameter (d_2, the contaminating fiber in Case B). Curves are labeled by the MCD calculated for the single fiber potential in Case A.

to the left minimum. As has been shown, the amplitude of the first minimum depends on the difference between fiber diameters, hence it is expected that it may prove useful for the present purpose.

A new method of fiber diameter determination

It has been shown by Zalewska et al. [32] that for SFP, it is possible to determine fiber diameter using the amplitude and negative peak duration. The area and NPD have been found to be the most suitable and sensitive parameters which may be used for this purpose. However, a graph similar to Fig. 7 can be constructed for other parameter pairs.

We were looking for a second pair of parameters such that the derived fiber diameter in case when the potential was contaminated by a second fiber was as distant as possible (in the sense of the determined fiber diameter) from the result obtained for the (amplitude, negative peak duration) pair.

We have calculated potentials and their parameters for fiber pairs. The primary fiber diameter was 35, 55, or 75 μm. The second fiber diameter was selected from within the allowed range with a step of 0.5 μm for the 55 and 75 μm cases and of 0.1 μm for the 35 μm case. The first fiber distance from the electrode was kept constant at 50 μm and the second fiber distance from the electrode ranged from 50 μm to 1000 μm. Altogether, about 250 contaminated potentials were calculated and their parameters were determined.

For each of these potentials, their false single fiber diameters were calculated using the amplitude-negative peak pair of parameters and a second trial pair of parameters. A sum of differences between the determined fiber diameters using these two pairs of parameters was calculated.

The calculations were performed for all available candidate pairs and it was found that the largest differences were obtained for a pair of R/L and area.

A graph similar to Fig. 7 but for R/L and area is shown on Fig. 10.

From this figure it is seen that when a second fiber is present within a distance of up to 250 μm from the electrode, it starts to affect significantly the derivation of fiber diameter. As may be seen, when the second fiber approaches the first one it leads to a progressively larger estimated fiber diameter. Thus, the effect of an addition of a second fiber on the estimated fiber diameter is opposite to that seen in the amplitude — NPD graph (Fig. 7).

As may be seen from Fig. 10, when the second fiber is close (second fiber to electrode distance of 50 μm), the single fiber diameter would have to be much larger than 95 μm. This makes it easy to detect unrealistic potential parameters, thus improving the chances of detecting a two fiber potential.

If the pairs (amplitude, negative peak duration) and (R/L, area) are used for single fiber potentials, then the fiber diameter determined from both of them was consistent. However, if the potential is due to two fibers then both determinations gave different results. Hence, using these two pairs it is possible to verify whether the potential may be due to a single fiber or whether it may be contaminated.

In order to illustrate the above statement, model potentials were calculated resulting from two fibers. The first fiber (of diameter $d1 = 55 \mu m$) was located at a distance of $r1 = 50 \mu m$ from the electrode and the second fiber had a diameter of $d2 = 53 \mu m$ and its distance from the electrode varied in the range of $50 \mu m \leq r2 \leq 800 \mu m$. Potential parameters including amplitude, negative peak duration, R/L and area were calculated from the resulting potential and the two estimates of fiber diameter were obtained using pairs (amplitude, negative peak duration) and (R/L and area). The estimates of fiber diameter based on these parameters were obtained from the interpolation in the set of single fiber model potentials calculated by us. The values of the two estimates of fiber diameter which are obtained by assuming that the recorded SFP is due to a single fiber are drawn in Fig. 11.

As may be seen from Fig. 11, when the second fiber is far away from the electrode ($r2 > 450 \mu m$), its perturbing
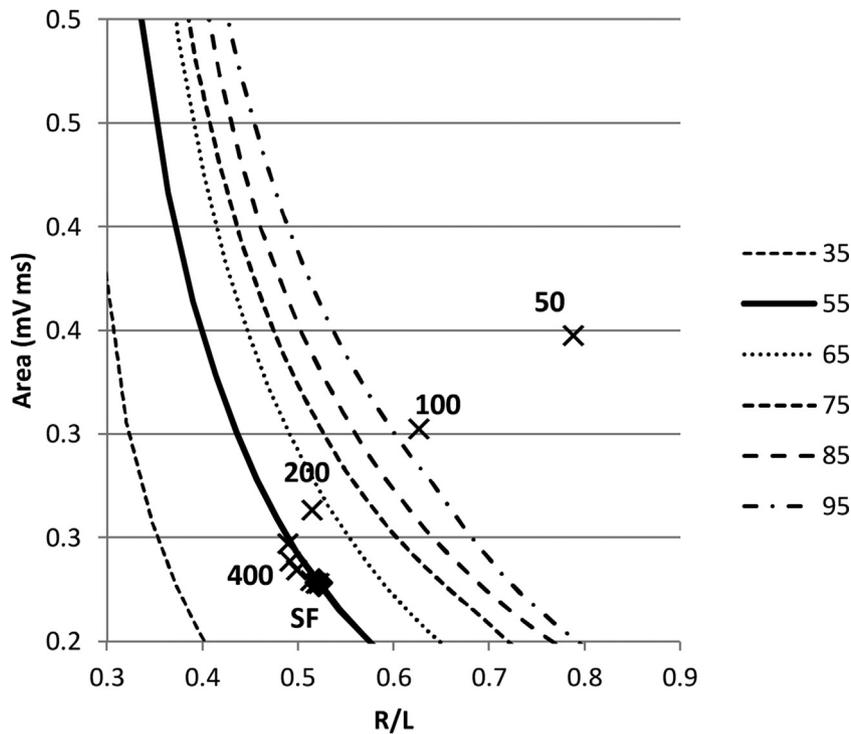
Figure 10 Determination of fiber diameter from R/L and area. The SF is the diameter of a fiber derived from single a fiber potential (55 μm diameter). The crosses are labeled with the distance of the second fiber from the electrode (in μm). The constant diameter curves obtained from the R/L vs. area relation are shown for diameters ranging from 35 μm to 95 μm.
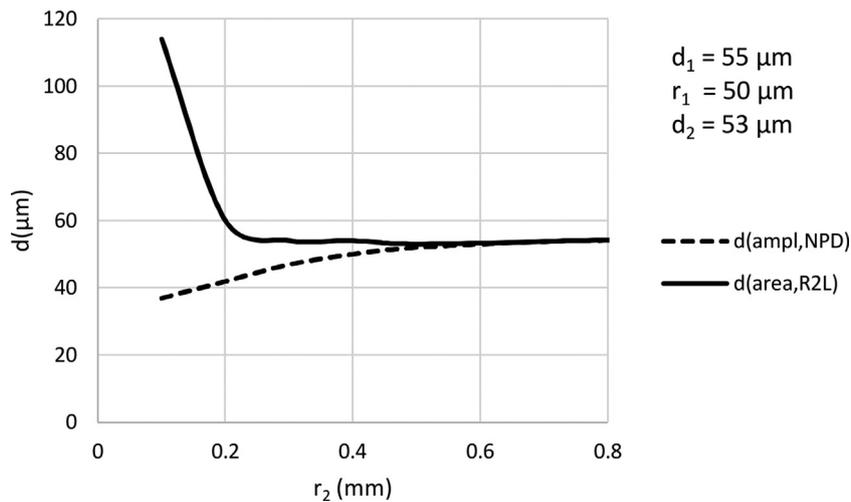
Figure 11 Fiber diameter estimates obtained using (amplitude, NPD) and (R/L, area) pairs of parameters in case when the potential is affected by the presence of a second fiber. When the second fiber is within the scoop range, the two estimates start to diverge enabling detection of a non SFP potential. See also text for description.

effect on the shape and parameters of the MUP becomes insignificant. For very large $r2$, the fiber diameter determined from both pairs of parameters becomes identical. This illustrates the fact that for a very large second fiber distance, the potential in effect becomes a SFP because the effect of the second fiber on the potential becomes negligibly small.

When the second fiber is moved closer to the electrode ($r2 < 450\,\mu m$), the fiber diameter obtained using

(amplitude, negative peak duration) tends to decrease, while the fiber diameter estimate obtained from (R/L and area) tends to increase rapidly. When the second fiber is, for example, at the distance of $100\,\mu m$ from the electrode, the two estimates of fiber diameter are $37\,\mu m$ and $114\,\mu m$. So, as it may be seen, even at a moderate distance from the electrode the second fiber does not have a significant effect on the potential shape and thus potential parameters.

The graph Fig. 11 also illustrates the efficiency of our method, as the sets of potential parameters used to determine the fiber diameter estimates were chosen in such a way as to give contradictory estimates in the presence of a second fiber, thus enabling verification whether the analysed MUP is due to a single fiber or not. For second fiber distances smaller than about 450 μm, the two methods give divergent estimates. At the distance of the second fiber of $r2 \approx 250\,\mu m$ the fiber diameters determined by the two methods give estimates that are different by more than 10% of the first fiber diameter. This shows that the method can detect the presence of a second fiber even at a distance from the electrode, and thus it is very sensitive.

Figs. 9 and 10 may be considered as a new constraint: in addition to the four criteria given in Introduction that a potential needs to meet in order to be classified as an SFP, the diameter estimates obtained using (amplitude, NPD) (Fig. 9) and (area, R/L) (Fig. 10) need to be in agreement in order for the potential to be classified as SFP.

Results similar to those obtained with the use of the new parameter R/L may be obtained using conventional pair of parameters: signal equivalent width equal to the area/amplitude and area. However, the method using equivalent width and area is about a thousand times less sensitive than the method using R/L and area. Hence, it is recommended that the parameter R/L is used for this purpose.

Discussion

Our analysis of the criteria defined for SFP verification suggests that there are two possible situations in which a potential recorded using a single fiber electrode may be misclassified, i.e., in case of a small fiber diameter and in case of contamination with a second fiber potential. The criteria (a) through (d) used to define a SFP tend to eliminate SFPs from small fibers. It has been shown (see Fig. 2) that with the rise time and amplitude criteria, SFPs may be detected only from fibers larger than about 30 μm. In the case of small fibers, with diameters between 30 μm and 40 μm, the fiber has to lie close to the electrode to be detected as SFP. Larger fibers may be more distant up to the distance of about 350 μm from the electrode.

It has been found that if the fibers in the motor unit have similar diameters (within few percent), they may form a potential that looks like a SFP. The conventional criteria (a) through (d) are insufficient to eliminate such cases. Therefore, care has to be taken to ascertain that a recorded potential is really a SFP.

We have examined consequences of a second fiber contaminating the potential and found that the second fiber may be quite far (more than 350 μm) away from the electrode and still affect the resulting potential.

When the second fiber is at a smaller distance, it leads to significant changes of the amplitude of SFP (but still within the limits given by (a)) and negative peak duration. These changes affect the method of determining the fiber diameter and fiber to electrode distance from SFP.

Since for standard fiber density there is about a 90% chance that two fibers will occur within the radius of 450 μm from the electrode, it is necessary to find a method that may be used to verify fiber diameter determination.

Rodriguez et al. have also studied the shape variability of potentials measured with a single fiber needle and found that the rise time variability is a sensitive indicator of whether the shape of the second peak is stable or not [18—21]. Our results corroborate their findings that in some cases, the presence of the second fiber may lead to either notch in the negative peak or an inflection in the rising part. The first case is routinely eliminated from the studies but the second is not (see Rodriguez for a discussion of type IV set). Both of these cases are due to the second fiber being of sufficiently different diameter. We observed (see Fig. 10) that even if the second fiber diameter is close to the diameter of the main fiber responsible for the second peak, so there would be no noticeable inflection or splitting of the second peak, the second fiber nevertheless has a significant effect on the calculated inter-spike duration. This is due to the fact that if two fibers contribute to the second peak, the jitter affects them in different ways. In the case of the second peak being due to a single fiber, the jitter will shift the second peak shape in time. In the case of the second peak being caused by two fibers, the shift in shape would (statistically) be expected to be smaller because for two fibers with close diameters, there will be cases where both fibers would be subject to the jitter of opposing direction. In the case of two fibers with similar diameters, the effect of the second (contaminating) fiber could manifest itself not in the increase of rise time variability but also in the change of the variability of the negative peak width. Both our study and the study by Rodriguez et al. [20] show that when considering jitter, care has to be taken to avoid contamination of the primary or secondary peaks by other fibers as this leads to significant changes of the determined average inter-spike duration.

The results of our study explain the possible influence of the contamination with other fiber potentials and therefore can be considered in respect to the jitter measurement. This might be of importance in cases of mild symptoms of abnormal neuromuscular transmission, and in cases of borderline jitter values. The impact of contributing fibers may result in a shift towards a negative or less frequently positive results and therefore may have clinical implications due to underestimation of the result.

We found that SFP criteria prevent detection of SFP from fibers smaller than about 30 μm in diameter, but do not prevent classification of a potential as an SFP even though it is formed by two or more fibers. This suggests that the presently used criteria may lead to incorrect interpretation of SFP potentials.

SFP contaminated by fibers of diameters differing by a few percent fulfill the criteria (a) through (d) but a negative peak may be shifted in time and therefore impact jitter and diameter measurements. The contamination tends generally to decrease the jitter as well as the determined diameter.

The results of this study may be also of importance for evaluation of the accuracy of jitter measurement using concentric needle (CNE) electrodes which are more prone to artifacts than single fiber EMG recordings. With voluntary activation, errors are caused by poor signal quality; inappropriate time reference points on the signal; an irregular firing rate; and signals with dual latencies [27]. For SFEMG jitter measurements, it is essential to record from well-separated

individual spikes, each generated by one muscle fiber. The CNE signal may be more complex due to superimposition of signals from different motor units. With voluntary activation, potentials from individual motor units are activated at different times, i.e., asynchronously. The short rising time without notches or shoulders and parallel rising phases on consecutive discharges are recommended as general criteria for CNE jitter [27]. In CNE jitter, the influence of contaminating components from distant fibers may increase potential asynchrony. The contamination tends generally to decrease the jitter as well as the determined diameter. The results of our study seem to be consistent with clinical observations that summated signals may have less jitter than single muscle fiber action potentials [24] (the jitter values for a voluntarily activated extensor digitorum communis using SFE ranged from 27.7 to 40.9 μs [4,11], while using CNE ranged from 23.3 to 30.7 μs) [9,12,25].

In summary, we have analysed properties of triphasic SFPs and proposed a new approach to the identification of SFP that determines the fiber diameter and distance from the electrode, in order to enable maximum sensitivity regarding potential contamination by an effect of a second fiber. Our findings allow identification of potentials that are contaminated by the presence of a second fiber, thus eliminating spurious potentials from the analysis of SFP and potential parameters based on SFP measurements. The proposed method of SFP determination is much more accurate than the currently adopted one based on the classical criteria (a) through (d) given in the Introduction.

Disclosure of interest

The authors declare that they have no competing interest.

References

[1] Arabadzhiev TI, Dimitrov GV, Chakarov VE, Dimitrov AG, Dimitrova NA. Effects of changes in intracellular action potential on potentials recorded by single-fiber, macro and belly-tendon electrodes. Muscle Nerve 2008;37:700—12.

[2] Bertorini TE, Stålberg E, Yuson CP, Engel WK. Single fiber electromyography in neuromuscular disorders: Correlation of muscle histochemistry, single-fiber electromyography and clinical findings. Muscle Nerve 1994;7:345—53.

[3] Blijham PJ, Laak HJ, Schelhaas HJ, van Engelen BG, Stegeman DF, Zwarts MJ. Relation between muscle fiber conduction velocity and fiber size in neuromuscular disorders. J App Physiol 2006;100:2233—41.

[4] Bromberg MB, Scott DM. Single fiber EMG reference values: reformatted in tabular form. AD HOC Committee of the AAEM Single Fiber Special Interest Group. Muscle Nerve 1994;17:820—1.

[5] Buchthal F, Guld C, Rosenfalck P. Action potential parameters in normal human muscle and their dependence on physical variables. Acta Physiol Scand 1954;32:200—18.

[6] Dumitru D, King JC, van der Rijt W, Stegeman DF. The biphasic morphology of voluntary and spontaneous single muscle fiber action potentials. Muscle Nerve 1994;17:1301—7.

[7] Ekstedt J, Nilsson G, Stålberg E. Calculation of the electromyographic jitter. J Neurol Neurosurg Psychiatry 1974;37:526—39.

[8] Ekstedt J. Human single fibre action potentials. Extracellular recording during voluntary and chemical activation. With some comments on end-plate physiology and on the fiber arrangement of the motor unit. Acta Physiol Scand 1964;Suppl 226:1—96.

[9] Erta M, Baslo MB, Yildiz N, Yazici J, Oge AE. Concentric needle electrode for neuromuscular jitter analysis. Muscle Nerve 2000;23:715—9.

[10] Gath I, Stålberg E. Frequency and time domain characteristics of single muscle fibre action potentials. Electroencephalogr Clin Neurophysiol 1975;39:371—6.

[11] Gilchrist JM, Barkhaus JE, Bril V, Daube J, DeMeirsman J, Howard JF, et al. Single fiber EMG reference values: a collaborative effort. Muscle Nerve 1992;15:151—61.

[12] Kouyoumdjian JA, Stålberg E. Concentric needle single fiber electromyography: normative jitter values on voluntary activated Extensor Digitorum Communis. Arq Neuropsiquiatr 2007;65:446—9.

[13] Merletti R, Parker PA. Electromyography, physiology, engineering and noninvasive applications. Wiley & Sons Publ; 2004.

[14] Nandedkar SD, Stålberg E. Simulation of single fiber action potentials. Med Biol Eng Comput 1983;21:158—65.

[15] Padua L, Stålberg E, LoMonaco M, Evoli A, Batocchi A, Tonali P. SFEMG in ocular myasthenia gravis diagnosis. Clin Neurophysiol 2000;111:1203—7.

[16] Preston DC, Shapiro BE. Electromyography and Neuromuscular Disorders. Clinical-Electrophysiologic Correlations. Elsevier Saunders; 2013.

[17] Rodriguez-Falces J, Gila L, Dimitrova NA. The morphology of single muscle fibre potentials — Part II: Experimental findings. J Electromyogr Kinesiol 2013;23:24—32.

[18] Rodriguez J, Malanda A, Gila L, Rodriguez I, Navallas J. Identification procedure in a model of single fibre action potential-part I: estimation of fibre diameter and radial distance. J Electromyogr Kinesiol 2010;20:264—73.

[19] Rodriguez J, Malanda A, Gila L, Rodriguez I, Navallas J. Identification procedure in a model of single fibre action potential-part II: global approach and experimental results. J Electromyogr Kinesiol 2010;20:274—83.

[20] Rodriguez-Falces J, Gila L, Dimitrova NA. Evaluation of the criteria to identify single-fibre potentials in human muscle fibres. Biol Cybern 2012;106:323—38.

[21] Rodriguez J, Navallas J, Gila L, Rodriguez I, Malanda A. Relationship between the rise-time of single fibre action potentials and radial distance in human muscle fibres. Clin Neurophysiol 2010;121:214—20.

[22] Sanders DB, Howard Jr JF. AAEE minimonograph #25: single-fiber electromyography in myasthenia gravis. Muscle Nerve 1986;9:809—18.

[23] Sanders DB, Stålberg EV. AAEM minimonograph #25: single-fiber electromyography. Muscle Nerve 1996;19:1069—83.

[24] Sanders DB. Clinical impact of single-fiber electromyography. Muscle Nerve Suppl 2002;11:15—20.

[25] Sarrigiannis PG, Kennett RP, Read S, Farrugia ME. Single-fiber EMG with a concentric needle electrode: validation in myasthenia gravis. Muscle Nerve 2006;33:61—5.

[26] Stålberg E, Sanders DB. Jitter recordings with concentric needle electrodes. Muscle Nerve 2009;40:331—9.

[27] Stålberg E, Sanders DB, Kouyoumdjian JA. Pitfalls and errors in measuring jitter. Clin Neurophysiol 2017;128:2233—41.

[28] Stålberg E, Trontelj J. Single fiber electromyography, Old Woking. United Kingdom: Mirvalle Press; 1979.

[29] Stålberg E, Sanders DB, Ali S, Cooray G, Leonardis L, Löseth S, et al. Reference values for jitter recorded by concentric needle electrodes in healthy controls: a multicenter study. Muscle Nerve 2016;53:351—62.

[30] Stålberg E. Single-Fiber EMG and Macro EMG An AAEM Demonstration. Workshop of American Association of Neuromuscular Electrodiagnostic Medicine; 2003.

[31] Zalewska E, Gawel M. Influence on jitter measurement from distant fibres in potential recorded by single-fibre electrode. Acta Physiol 2017;e12994:1—3.

[32] Zalewska E, Nandedkar SD, Hausmanowa-Petrusewicz I. A method for determination of muscle fiber diameter using single fiber potential (SFP) analysis. Med Biol Eng Comp 2012;50:1309—14.

[33] Zalewska E. Deriving muscle fiber diameter from recorded single fiber potential. Neurophysiol Clin 2017;47:413—7.